Chemosphere 364 (2024) 143131

Contents lists available at ScienceDirect

Chemosphere

journal homepage: www.elsevier.com/locate/chemosphere

Photoaging of polystyrene-based microplastics amplifies inflammatory response in macrophages

Noemi Aloi [a], Anna Calarco [b], Giusy Curcuruto [c], Marilena Di Natale [d], Giuseppa Augello [a], Sabrina Carola Carroccio [c], Pierfrancesco Cerruti [e], Melchiorre Cervello [a], Angela Cuttitta [d], Paolo Colombo [a,*], Valeria Longo [a]

[a] Institute for Biomedical Research and Innovation, National Research Council of Italy (IRIB-CNR), Via Ugo La Malfa 153, 90146, Palermo, Italy
[b] Research Institute on Terrestrial Ecosystems, National Research Council of Italy (IRET-CNR), Via P. Castellino 111, 80131, Napoli, Italy
[c] Institute of Polymers, Composites and Biomaterials, National Research Council of Italy (IPCB-CNR), Via Paolo Gaifami 18, 9, 95126, Catania, Italy
[d] Institute for Studies on the Mediterranean, National Research Council of Italy (ISMED-CNR), Via Filippo Parlatore 65, 90145, Palermo, Italy
[e] Institute of Polymers, Composites and Biomaterials, National Research Council of Italy (IPCB-CNR), Via Campi Flegrei 34, 80078, Pozzuoli, Italy

HIGHLIGHTS

- Physical characterization of pristine and aged polystyrene microparticles.
- Immunological performances of pristine and aged polystyrene microparticles.
- Cytotoxicity, oxidative stress, genotoxicity and inflammatory responses.

GRAPHICAL ABSTRACT

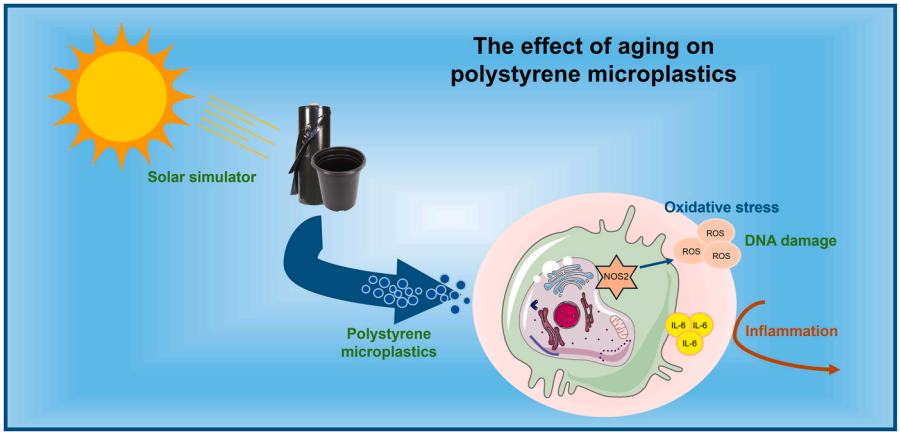

ARTICLE INFO

Handling editor: Alvine C.Mehinto

ABSTRACT

The continuous release of municipal and industrial products into the environment poses a growing concern for public health. Among environmental pollutants, polystyrene (PS) stands out as a primary constituent of environmental plastic waste, given its widespread use and high production rates owing to its durability and user-friendly properties. The detection of polystyrene microparticles (PS-MPs) in various living organisms has been well-documented, posing a serious threat due to their potential passage into the human ecosystem. In this manuscript, we aimed to study the toxicological effects of low concentrations of pristine and photoaged PS-MPs in a murine macrophage cell line. To this purpose, PS-MPs were photoaged by indoor exposure to visible light to

* Corresponding author. Istituto per la Ricerca e l'Innovazione Biomedica (IRIB) del Consiglio Nazionale delle Ricerche Via Ugo La Malfa, 153 90146, Palermo, Italy.
E-mail address: paolo.colombo@irib.cnr.it (P. Colombo).

https://doi.org/10.1016/j.chemosphere.2024.143131
Received 9 May 2024; Received in revised form 30 July 2024; Accepted 17 August 2024
Available online 19 August 2024

simulate environmental weathering due to solar irradiation (PS-MPs^{3h}). Physical characterization revealed that the irradiation treatment results in particle degradation and the possible release of nanoparticles. Monocultures of the RAW264.7 cell line were then exposed to PS-MPs and PS-MPs^{3h} at concentrations comparable to experimental measurements from biological samples, to assess cytotoxicity, intracellular oxidative stress, primary genotoxicity, and inflammatory effects. Significant toxicity-related outcomes were observed in cells treated with both pristine PS-MPs and PS-MPs^{3h} even at low concentrations (0,10 μg/ml and 1 μg/ml). PS-MPs^{3h} exhibited greater adverse effects compared to PS-MPs, including reduced cell viability, increased ROS production, elevated DNA damage, and upregulation of IL-6 and NOS2 gene expression. Therefore, we can conclude that changes induced by environmental aging in the physicochemical composition of PS microplastics play a crucial role in the adverse health outcomes associated with microplastic exposure.

1. Introduction

The exponential growth of the world economy has led to increased resource exploitation and industrial production, resulting in a significant transfer of contaminants into the environment, which has had various impacts on public health. In the European Union, an estimated 30 million people, constituting about 6% of the total European population, reside near landfills (Shaddick et al., 2018). Moreover, an estimated 2.5 million contaminated sites exist across Europe, potentially leading to significant adverse health effects caused by the dispersion of various substances resulting from human activities. Over time, microplastics (MPs), measuring less than 5 mm in size, generated through the degradation of plastic waste via physicochemical processes in the environment, have emerged as a novel pollutant and emerging global concern (Kumar et al., 2021). Due to their small size and ubiquitarian occurrence in the aquatic environment (Eriksen et al., 2014; Horton et al., 2017), MPs are potentially bio accessible for a wide range of biotas (Wang et al., 2016) showing multiple adverse effects on marine organisms (Wagner et al., 2014; Eerkes-Medrano et al., 2015; Wright and Kelly, 2017). The presence of MPs in food destined for human consumption and in air samples has been reported (Usman et al., 2020; Cunningham et al., 2022). MPs were observed in the totality of 16 different species of fish, squid, and shrimp, all of human consumption (Alfaro-Nunez et al., 2021) and several types of MPs have been detected in human faeces (Schwabl et al., 2019). Indeed, microplastics can not only negatively affect the ecosystem itself, but due to their large specific area and strong hydrophobicity can also easily interact with a plethora of hydrophobic organic pollutants, heavy metals, and pathogens, which leads to serious environmental problems (Hodson et al., 2017; Huang et al., 2021). Microplastics exhibit considerable variability in chemical composition, size, and shape, all of which can influence exposure levels, as well as local or systemic uptake, and cellular and molecular interactions with the plastics. Polystyrene (PS) is a major contributor to MP contamination because expanded polystyrene (EPS), commonly used in insulation and packaging, easily forms and releases MPs into the environment through littering and environmental degradation. Nonetheless, the styrene monomer present in PS is a known carcinogen, posing a potential threat to organisms (Frank and Meek, 2024). So far, toxicity studies on PS rely on *in vivo* model organisms and large set of MPs, revealing potential toxicity following ingestion and subsequent accumulation in various tissues (Hou et al., 2021; Jin et al., 2021). Several studies evidenced that the photo-oxidative degradation process occurring upon environmental exposure plays an important role in determining the environmental behaviour of MPs (Andrady, 2015). Di Natale and coworkers found that UV photo exposure led to a significant decrease in molecular weight, sphericity loss, and surface deformation of polystyrene microplastics (Di Natale et al., 2022). Mao and coworkers also highlighted that UV irradiation under different conditions changes the physicochemical properties of PS-MPs since their surface appears rough and crystallinity and oxygen-containing groups on the surface increase (Mao et al., 2020). To date, in the current research on MP environmental transformation, most research has been focused on the sorption of chemical contaminants on MPs after UV photo-exposure (Rodrigues et al., 2019), as well as on its effects on MPs' degradation and breakage rate (Cai et al., 2018; Liu et al., 2019). The extent to which these environmental factors modify the biological interactions and health risks associated with microplastics remains unclear. It has been demonstrated that microplastic particles can induce cellular toxicity through mechanisms such as oxidative stress, membrane damage, immune response, and genotoxicity (Fleury and Baulin, 2021). Once microplastics are inhaled or ingested, they may accumulate and trigger an immune response, potentially leading to localized particle toxicity (Wright and Kelly, 2017). Nevertheless, the majority of the above presented evidence primarily stems from cell exposure to MP concentrations far exceeding those found in natural environments, potentially undermining its applicability to real-world scenarios. Therefore, in this manuscript, we specifically studied the effects of visible light (VL) irradiation on polystyrene microplastics at concentrations levels typically detected in environmental conditions and, downstream, the effects on macrophage viability and functionality using the murine macrophage cell line RAW264.7.

2. Methods

2.1. Reagents

Additive-free polystyrene microparticles (PS-MPs) [mean size of 1,01 μm, cat. N° PP10-10-100 Spherotech Inc. (IL-USA)].

2.2. Preparation and aging of PS-MPs

An aliquot of PS-MPs suspension (500 μL of SPHERO™ polystyrene microparticles water dispersion 10% W/v) was placed in a sterilized Petri dish, frozen and lyophilized. Then, PS-MPs were irradiated by using the VeraSol-2 device (Oriel, Newport) for 3 h. The VeraSol-2 is a simulator of Class AAA with LED lamps with adjustable Output Power from 0.1 to 110 mW/cm^2. Oriel put each LED-based system to rigorous testing for all aspects of standards to ensure compliance and provides a certificate of calibration over 10.000 h (https://www.newport.com/p/VeraSol-2). In our experiments, the irradiation corresponds to AM 1.5 G works in the visible and near-infrared region (400–1100 nm) with a light irradiance of 100 ± 3 mW/cm^2.

2.3. Characterization of PS microparticles

Chemical characterization of pristine and aged PS-MPs was carried out by Gel Permeation Chromatography (GPC) and Matrix-Assisted Laser Desorption Ionization-Time of Flight (MALDI-TOF). For GPC, 3 mg of PS-MPs were dissolved in 1 ml of tetrahydrofuran (THF), which was also used as eluent. Molar masses values were determined using Azura GPC Knauer and THF (see Supplementary material section Fig. S1).

For MALDI-TOF analysis, PS-MPs and PS-MPs^{3h} solutions were analyzed in reflector mode with an UltrafleXtreme MALDI TOF/TOF AB Sciex instrument. Solvent and matrix were selected after testing at least three MALDI recipes from the National Institute of Standards and

Technology (NIST) Synthetic Polymers MALDI Recipe Database (https://maldi.nist.gov/). The best matrix/solvent combination for our material in terms of signal-to-noise ratio was IAA/THF, as described in the supporting information (see Supplementary material section Figs. S2 and S3, respectively). The acquired data were processed using FlexAnalysis software.

Furthermore, the behaviour of pristine and aged PS-MPs in aqueous suspension was studied by Dynamic Light Scattering (DLS) and Nanoparticles Tracking Analysis (NTA).

Since the ionic strength and pH of the solution can impact the results obtained through DLS and NTA differently, making direct comparison of the results potentially difficult, we chose to compare NTA and DLS data only in the case of PS-MPs and PS-MPs^{3h} water solutions. To this aim, 100 μL of microparticle aqueous suspension (50 μg/ml) were added to 2 mL of H_2O, and then analyzed by DLS and NTA, using Malvern ZS and NanoSight instruments, respectively (see Supplementary material section for further details). The effect of DMEM on particle size, polydispersity, and agglomeration was evaluated by DLS using the same procedure used with H_2O.

2.4. Cell line cultures

Murine macrophage RAW264.7 were purchased from ATCC (#TIB-71 Rockville, MD, USA). Cells were cultured in semi-adherence in Dulbecco's Modification of Eagle's Medium – high glucose (High DMEM, Corning, Milan, Italy, cat. 10-101-CV) supplemented with heat inactivated 10% Foetal Bovine Serum (FBS, Gibco Life Technologies, cat. 10270106) and 100 U/mL penicillin and 100 μg/mL streptomycin (Sigma-Aldrich, Milan, Italy; cat. P4333). Cells were treated with PS-MPs and PS-MPs^{3h} after overnight adhesion at 37 °C and 5% CO_2.

2.4.1. MTS assay

Cell viability was determined *in vitro* by 3-(4,5-dimethylthiazol-2-yl)-5-(3-carboxymethoxyphenyl)-2-(4-sulfophenyl)-2H-tetrazolium) MTS assay, using the kit CellTiter 96® Aqueous One Solution Cell Proliferation Assay (Promega, USA; cat. G358B) and according to the manufacturer's protocol. The RAW264.7 cells were seeded at a concentration of 25000 cells/well in 96-wells tissue culture plates and treated with different concentrations of PS-MPs or PS-MPs^{3h} (0.01 μg/mL, 0.1 μg/mL, 1 μg/mL and 10 μg/mL) in complete high glucose DMEM medium for 24 h and 48h. At the defined time point, 15 μL of MTS solution was added, and the cells were further incubated for an additional 2 h in dark conditions. The absorbance of the dissolved formazan was measured in an automated microplate reader (Imark Plate Reader - BioRad) at 490 nm. According to the manufacturer's protocol cell viability percentage was determined as the ratio between the absorbance (O.D.) of treated and control cells x 100. Control cells were defined as non-treated cells (NT). Data were represented as means ± SD of three experiments, each in triplicate. Comparisons were made using the one-way ANOVA multiple comparisons test.

2.4.2. Measurement of ROS production

RAW264.7 cells were seeded at a concentration of 25000 cells/well in 96-wells tissue culture plates and treated with different concentrations of PS-MPs or PS-MPs^{3h} (0.1 μg/mL, 1 μg/mL) for 24h. Lypopolysaccharide (LPS) 1 μg/mL (E. coli serotype O26:B6, Sigma-Aldrich, Milan, Italy; cat. L5543) was used as positive control. For each time of treatment, cells were washed with 50 μL of 1X PBS w/o Ca^{2+} and Mg^{2+} and incubated with 10 μM of 2′,7′-Dichlorofluorescin Diacetate (DCF-DA) (Sigma-Aldrich, Milan, Italy, cat. D6883) for 3h in dark conditions. The relative ROS levels were quantified by measuring the fluorescence intensity at an excitation wavelength of 475 nm and an emission of 500–550 nm using a microplate reader (Glomax® Discover Microplate Reader, Promega, Milan, Italy). Data were obtained from three independent experiments, each in triplicate and results were expressed as percentage (%) of ROS vs control.

2.4.3. RNA isolation and gene expression analysis

The RAW264.7 macrophages were seeded at a density of 5×10^5/well in 24 wells tissue culture plates and cultured in High glucose DMEM medium supplemented with heat inactivated 10% Fetal Bovine Serum (Gibco, Life Technologies) and 1% antibiotic (penicillin 100 U/ml, Streptomycin sulfate 100 mg/ml, Invitrogen). After 24 h of incubation at 37 °C and 5% CO_2, cells were washed in 1X PBS w/o Ca^{2+} and Mg^{2+} and treated with two different concentrations (0.1 μg/mL and 1 μg/mL) of PS-MPs or PS-MPs^{3h} in the culture medium and incubated for 24 h at 37 °C and 5% CO_2. Total RNAs were extracted according to the manufacturer's protocol of RNeasy Mini kit (Qiagen, Milan, Italy) and the cDNA synthesis was performed using the QuantiTect Reverse Transcription Kit (Qiagen, Milan, Italy). The Real Time analyses were performed by the Applied Biosystems StepOnePlus™ Real Time PCR System and the Sybr Green technology. Real time reactions were performed using 1–100 ng of cDNA in 2X Fast Sybr Green Master mix (Applied Biosystems, Thermo Fisher Scientific, Milan, Italy) and 200 nM of specific mouse IL-6 (NM_031168) and NOS2 (NM_010927) primers (QuantiTect Primer Assays, Qiagen, Milan). The housekeeping gene used in all analyses was the mouse 18S ribosomal RNA (NR_003278). The amplification conditions were: initial denaturing step at 95 °C for 20 s followed by 40 cycles of two step PCR denaturation at 95 °C for 15 s and annealing/extension at 60 °C for 30 s.

2.4.4. Western Blotting

Radioimmunoprecipitation assay buffer (Cell Signaling Technologies Inc., Beverly, MA, USA) was used to obtain cell lysates, and Western Blotting was performed as previously described (Cusimano et al., 2015). Primary antibodies were diluted at 1:1000 in Odyssey® blocking buffer (OBB, LI-COR) and tris-buffered saline (TBS). γH2AX were obtained from Cell Signaling Technologies (Beverly, MA, USA) and β-actin were obtained from Merck (Milan, Italy). Secondary antibodies conjugated to IRDye® 800CW (LI-COR) or Alexa Fluor 680 (Molecular Probes, Invitrogen Carlsbad, CA, USA) were diluted at 1:10000 in OBB and TBS. Membranes were scanned and analyzed with an Odyssey IR scanner using Odyssey 3.0 imaging software.

2.4.5. Immunofluorescence

RAW264.7 cells were seeded in 96-well at a concentration of 25×10^3 cell/well and, after 24 h, were exposed to 0.1 μg/ml and 1 μg/ml of PS-MPs and PS-MPs^{3h}. At the end of treatment, cells were fixed in 4 % paraformaldehyde for 15 min at room temperature and washed 3 times with phosphate-buffered saline (PBS) and permeabilized with 0.2 % Triton X-100 in PBS for 10 min. Samples were then incubated in blocking solution of 5 % BSA in PBS for 10 min and subsequentlyincubated with the anti-γH2AX antibody (diluted 1:400, Cell Signaling) overnight at 4 °C. Cells were washed 3 times with 1X PBS and then incubated with fluorescein (FITC)-conjugated goat anti-rabbit (diluted 1:500, Alexa Fluor 488, Invitrogen). After washing, cells were then incubated with Hoechst 33342 for 30 min to visualize nuclei. Images were acquired and collected at 40× magnification using an Olympus fluorescent microscope (Olimpus Evident iX3).

2.4.6. Statistical analysis

Data are reported as means ± SD. Comparisons were made by performing the one-way ANOVA multiple comparisons test and two-way ANOVA or mixed model multiple comparisons test both with the Tukey method. Analyses were conducted using GraphPad Prism Version 8.0.2. Values were considered statistically significant when $p \leq 0.05$.

3. Results

3.1. GPC and MALDI TOF characterization of PS-MPs

The chemical characterization of PS-MPs was performed by GPC and MALDI TOF analyses. The GPC data, (see Supplementary Fig. S1),

showed Molar Masses with a PD higher than 2, denoting a typical radical polymerization process. Regarding MS analysis, the scarce amount of low molar fraction did not allow for obtaining high-resolved MALDI spectra. However, at low mass range (Supplementary Figs. S2 and S3), it is possible to assign peaks to macromolecular chains with different end groups (See Supplementary Table S1) (Carroccio et al., 2003).

3.2. NTA and DLS characterization of PS-MPs

Pristine and aged PS-MPs aqueous dispersions were characterized by NTA, to determine their concentration in water dispersion, and to assess the possible effect of UV irradiation on their size. In NTA, the scattered light from solution-dispersed particles impinged by a laser beam is captured by a microscope fitted with a camera, and software analysis tracks the Brownian motion of the particles to determine their hydrodynamic diameters using the Stokes-Einstein equation: D_t=(K_B T)/(6πηr_h)

where K_B is Boltzmann's constant, T is temperature and η is solvent viscosity (Urso et al., 2022). Notably, NTA has been applied to gauge nanoplastic concentrations in water samples and to monitor nanoplastic release resulting from the breakdown of microplastics (Park et al., 2005). Fig. 1 shows the concentration as a function of the size distribution for the PS-MPs before (panel a) and after photo ageing (panel b). Frames of the video recorded for the MPs dispersions are also provided in the figure, where the particles are traced as bright spots on a dark background.

PS-MP displayed significant size polydispersity, as confirmed by the presence of several peaks from 34 to 1000 nm diameter (Fig. 1 panel a). Their concentration was 3.3 ± 0.6 × 10^8 particles/mL, with a mean diameter of 456 ± 303 nm, while 90% of them were within 853 nm. The aging treatment did not affect the mean diameter of the NPs, which was found to be 465 ± 212 nm (Fig. 1 panel b). However, the 90-percentile value decreased to 754 nm, and the concentration slightly increased to 5.4 ± 0.4 × 10^8 particles/ml. This evidence suggests that the irradiation could result in particle degradation and the possible release of nanoparticles in the solution. To get further insights on this aspect, and to overcome the upper size limit of NTA (1000 nm), which is restricted by the limited Brownian motion of large particles, the PS-MPs and PS-MPs^{3h} water dispersions characterized by NTA were also analyzed by DLS. Additionally, DLS characterization was also performed on PS particles suspended in DMEM, and in DMEM supplemented with 10% Fetal Bovine Serum, coded as DMEM complete (Fig. 1 panels c and d). In both cases, DLS showed the occurrence of a single broad scattering peak in all suspending agents, because the scattering intensity from the larger species largely overcame that from the smaller ones, so that the latter were not detected by DLS (Argenziano et al., 2023). In the case of PS-MPs in water (Fig. 1 panel c), the average hydrodynamic diameter peaked at 1280 ± 311 nm, confirming that DLS should complement NTA when characterizing particles with average size in the range of 1000 nm. Upon ageing, the average hydrodynamic diameter slightly decreased to 1120 ± 241 nm, corroborating the evidence gathered from NTA about the degradation of the PS-MPs. Hydrodynamic diameter and polydispersity were measured also in DMEM, to get insight on the effect of the suspending medium on size and agglomeration of pristine and aged PS-MPs. When dispersed in DMEM, pristine PS-MPs and PS-MPs^{3h} tended to cluster, exhibiting increased size values, up to 1711 ± 405 and 1453 ± 275 nm, respectively. The introduction of 10% FBS in DMEM had a slight impact on the self-assembly behavior of PS-MPs, as the average size increased to 1731 nm for the pristine PS-MPs (Fig. 1 panel c), and even decreased in the case of PS-MPs^{3h}, from 1453 to 1422 nm (Fig. 1 panel d).

3.3. Cytotoxic effects of PS-MP^{3h} on murine macrophages

Cytotoxic effects of polystyrene microparticles were evaluated by means of MTS assays, using the RAW264.7 macrophage cell line. The assays were performed incubating cells with increasing concentrations (from 0.01 to 10 μg/mL) of either PS-MPs or PS-MPs^{3h} for 24 and 48 h. Data reported in Fig. 2 have shown that PS-MPs did not affect cell viability both at 24 h and 48 h of treatment, compared to control cells.

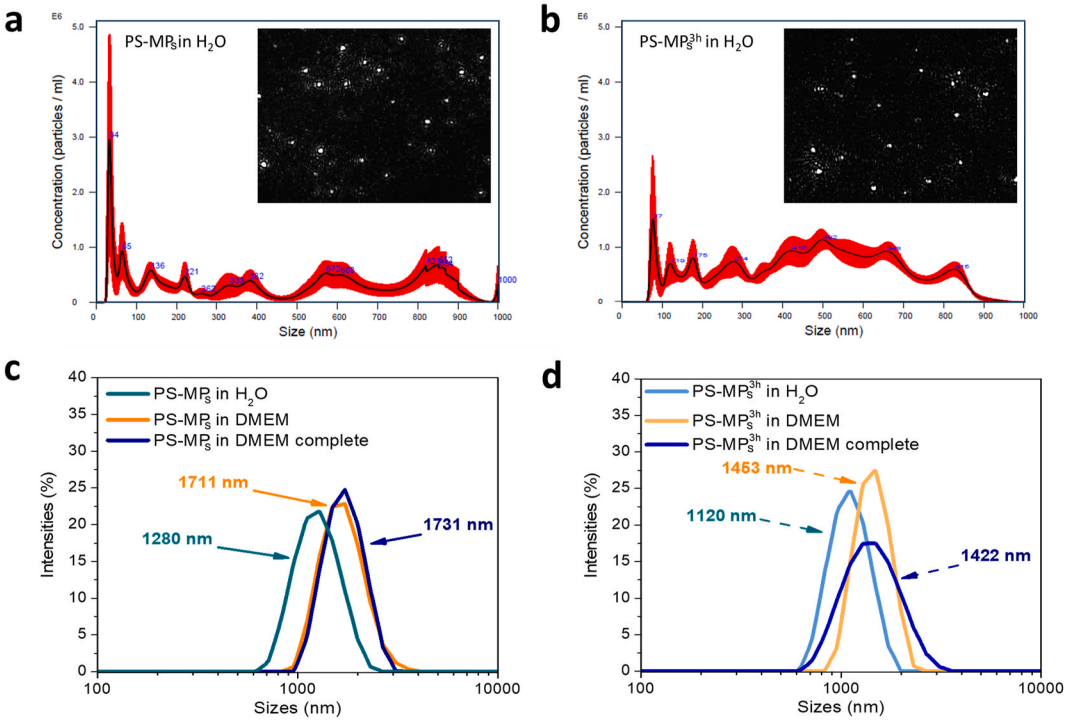

Fig. 1. NTA and DLS characterization of PS-MPs. Concentration *vs* size distribution of panel a) pristine PS-MPs, and panel b) PS-MPs^{3h} in water as measured by NTA. Insets in the figures display frames of the videos of PS-MPs suspensions. DLS results of panel c) neat PS-MPs, and panel d) PS-MPs^{3h} samples suspended in water, DMEM or DMEM complete. n = 3 independent replicates.

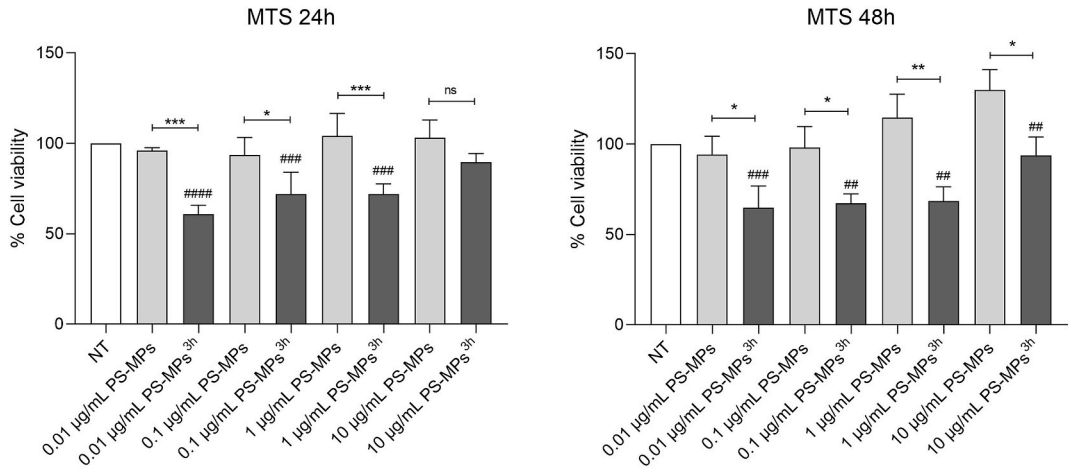

Fig. 2. *In vitro* cell viability assay. Cytotoxicity of RAW264.7 macrophage cell line measured by the MTS assay upon 24h (Panel A) and 48h (Panel B) treatment with PS-MPs and PS-MPs^{3h}. Data shows means ± SD of three experiments, each in triplicate.

Instead, PS-MPs^{3h} induces a drastic and statistically significant reduction in cell viability percentage both at 24 and 48 h of treatment. Specifically, it has been observed that compared to controls, PS-MPs^{3h} significantly reduces cell viability about of 30–40% at the concentrations of 0.01 µg/mL ($p < 0.0001$), 0.1 µg/mL ($p = 0.0007$) and 1 µg/mL ($p = 0.0007$). A similar result was obtained comparing the cell viability between samples treated with PS-MPs vs PS-MPs^{3h} for 24h and 48h at the concentrations of 0.01 µg/mL ($p = 0.0014$ and $p = 0.0397$, respectively), 0.1 µg/mL ($p = 0.0373$ and $p = 0.0167$, respectively) and 1 µg/mL ($p = 0.0028$ and $p = 0.0013$, respectively). The data were summarized in Fig. 2 panels A and B.

3.4. Evaluation of ROS production induced by PS-MPs^{3h} in murine macrophages

To evaluate whether polystyrene microparticles can induce oxidative stress mechanisms in macrophage cell line, the level of reactive oxygen species (ROS) production was analyzed in RAW 264.7 cells treated with PS-MPs and PS-MPs^{3h} by means of 2′,7′-Dichlorofluorescin Diacetate (DCF-DA) fluorescent probe. Macrophages were incubated with the same concentration of PS-MPs and PS-MPs^{3h} used in the cell viability assays and the percentage of ROS level determined by measurements of fluorescence intensity. The data reported in Fig. 3 showed that PS-MPs^{3h} significantly enhanced ROS production in RAW264.7 cells after 24h of treatment respect to pristine PS-MPs whose stimulus it is comparable to the untreated cells. This result suggested that PS-MPs^{3h} induce oxidative stress by producing ROS in the RAW264.7 cells.

3.5. Evaluation of DNA damage induced by PS-MPs^{3h} in murine macrophages

ROS production can result in DNA damage particularly in the form of DNA double strand breaks (DSBs) corroborated by the increase of phosphorylation of histone H2AX (Kuo and Yang, 2008). Thus, we investigated whether exposure to polystyrene microparticles could induce DNA damage in RAW 264.7 cells. As highlighted by immunofluorescence staining, we observed an increase of accumulation of γH2AX in the cell nucleus after PS-MPs and PS-MPs^{3h} at 0.1 µg/ml and 1 µg/ml (Fig. 4 panel A) after 24 h of treatment. Furthermore, γH2AX levels were determined by Western Blot after treatment with pristine and aged PS-MPs at the same reported concentrations. Fig. 4 panel B shows an increase in γH2AX in PS-MPs^{3h} treated samples compared to PS-MPs. Lipopolysaccharide stimulation was used as a DNA damage inducer control (Lee et al., 2017).

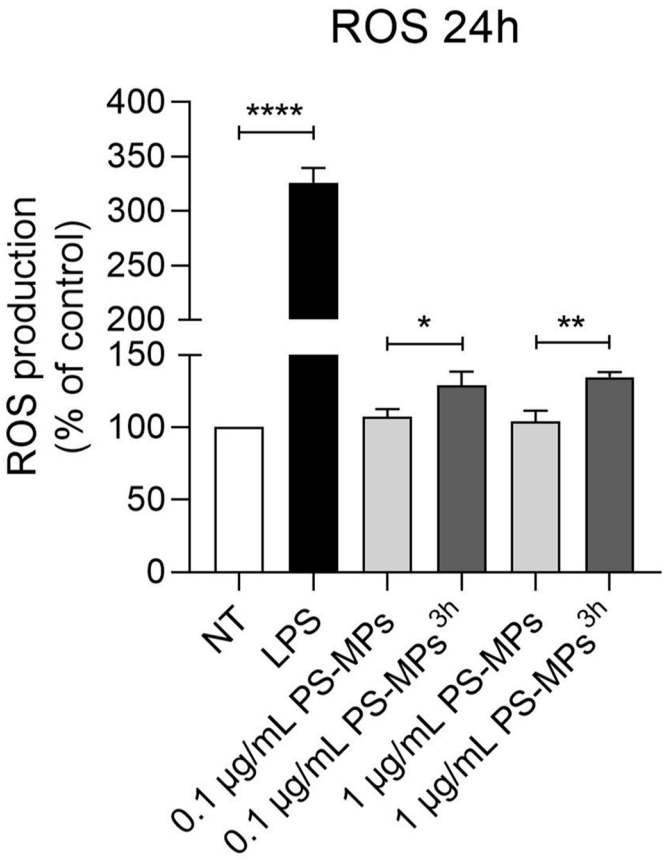

Fig. 3. ROS production of RAW264.7 cell line stimulated with PS-MPs and PS-MPs^{3h} for 24h. ROS production were expressed as percentage vs control (untreated cells). LPS [1 µg/mL] was considered as positive control. Data show means ± SD of three experiments, each in triplicate.

3.6. Impact of PS-MPs^{3h} on inflammatory cytokine and oxidative stress expression

To further study the inflammatory and oxidative effect of polystyrene microparticles on RAW264.7 cells, we investigated their effects on the expression of interleukin-6 (IL-6) and Nitric Oxide Synthase 2 (NOS2) after 24h of treatment with PS-MPs and PS-MPs^{3h} (0.1 μg/mL and 1 μg/mL). As shown in Fig. 5, murine macrophage incubated with

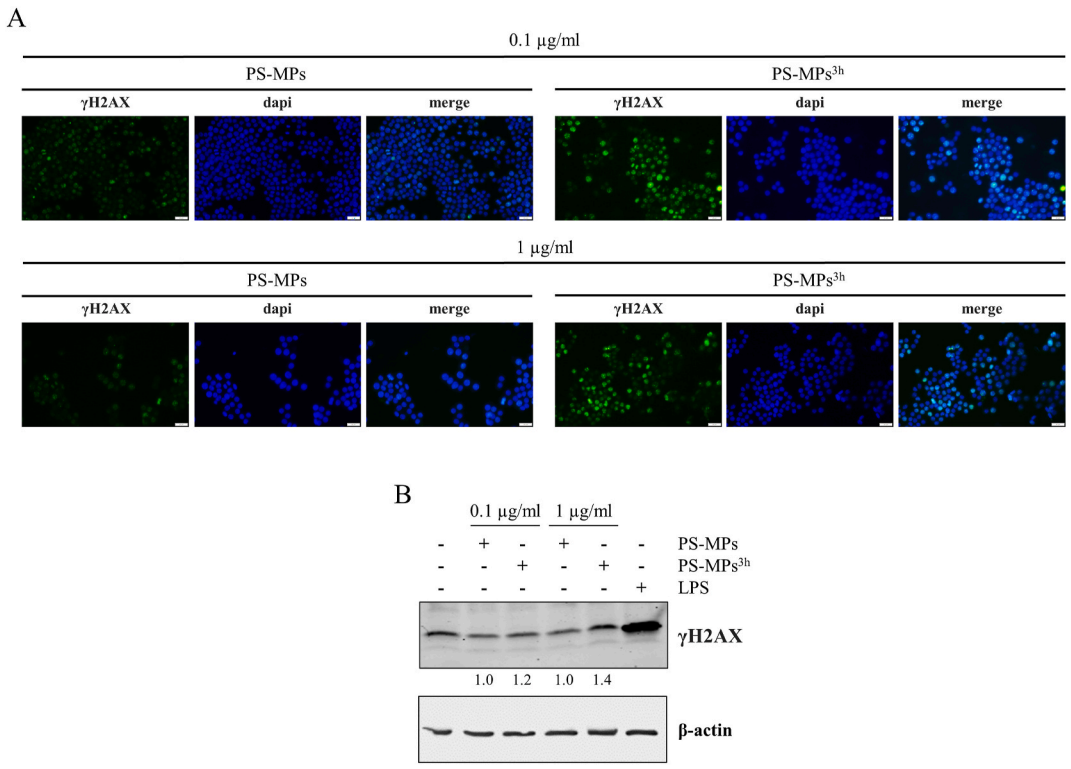

Fig. 4. Panel A. Immunofluorescence analysis of γH2AX protein expression after treatment of RAW 264.7 cells with 0.1 µg/ml or 1.0 µg/ml PS-MPs/PS-MPs^{3h}. Cells were exposed to the indicated microplastic (PS-MPs, PS-MPs^{3h}) at the concentrations of 0,1 and 1 µg/ml for 24 h. Panel B. Immunoblotting evaluation of γH2AX protein expression in RAW 264.7 cells after microplastic treatments. 1 µg/ml of LPS was used a positive control. The numbers represent the ratio of the relevant protein normalized with β-actin, with vehicle-treated control samples arbitrarily set at 1.0.

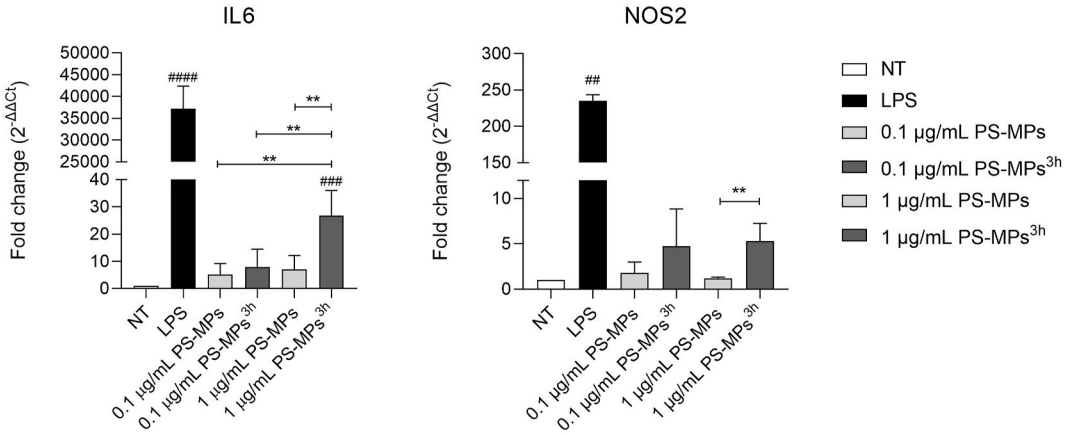

Fig. 5. qPCR analysis of IL-6 and NOS2 cytokine mRNAs in murine macrophage RAW264.7 cell line stimulated with PS-MPs and PS-MPs^{3h} for 24h. The gene expression was normalized respect to untreated cells (NT). Data shows means ± SD of three experiments, each in triplicate.

PS-MPs^{3h} showed an increase of expression of the pro-inflammatory cytokine IL-6 compared to stimulation with pristine PS-MPs at both concentrations and in a dose-dependent manner. A comparable trend can be observed in the up-regulation of NOS2 in with aged PS-MPs^{3h} respect to PS-MPs.

4. Discussion

Microplastics are ubiquitous environmental pollutants spread across different ecosystems and a growing body of evidence suggests that microplastics are being integrated into widely consumed food items (EFSA, 2021) via either animals ingesting microplastics in the environment (Santillo et al., 2017) or contamination during production and/or by plastic packaging (Sewwandi et al., 2023). Based on overall food consumption, Cox and coworkers (Cox et al., 2019) reported that annual microplastics consumption in humans ranges from 39000 to 52000 particles depending on age and sex. These estimates increase to 74000 and 121000 when inhalation is also considered. Among this large set of plastic products, polystyrene is one of the most frequently used plastic in the food industry. Studies have suggested that exposure to polystyrene particles can trigger inflammatory responses in the body (Heddagaard and Moller, 2020). When polystyrene is broken down into smaller particles, either through physical abrasion or environmental degradation (i.e. sunlight), these particles can be inhaled (Baeza-Martinez et al., 2022) or ingested (Covello et al., 2024; Visentin et al., 2024), leading to activation of the immune system (Fan et al., 2024). Innate immune system is

the first line of defence against xenobiotics and, in particular, macrophages are essential components of the innate immune system playing a critical role in responding to foreign particles and pathogens in the body. These specialized immune cells are equipped with a variety of receptors that enable them to detect and respond to foreign particles, including nanoparticles. Several papers analyzed the macrophage interactions with polystyrene particles offering insights into cellular responses, phagocytic processes, and the immunomodulatory effects of these synthetic materials on immune cells (Yang et al., 2022; Yin et al., 2023). Leslie and coworkers revealed the presence of approximately 1.6 μg/mL of plastics demonstrating that plastics are bioavailable for uptake in the blood (Leslie et al., 2022). Based on our observations (data not shown) and on this experimental evidence, we decided to investigate the biological effects of polystyrene microplastics at concentration ranges similar to those experimentally evaluated in human biological samples. To accomplish this task, commercially available polystyrene microparticles were irradiated in mild conditions by using the VL wavelength range (see experimental part) and then studied for their ability to modulate the proinflammatory response of murine macrophage RAW264.7 cell line. Macrophages can detect changes in the physicochemical properties of nanoparticles, such as size, shape, surface charge, and surface chemistry (Banerjee and Shelver, 2021; Jeon et al., 2023; Soni et al., 2024). These characteristics influence the interactions between nanoparticles and macrophages, affecting their recognition and internalization. Therefore, pristine and aged polystyrene particles were initially studied for their physical characteristics by means of GPC, MALDI-TOF, NTA, and DLS techniques to study the effect of the treatment on the size, number, and polydispersity of the PS-MPs *vs* PS-MPs^{3h} particles. As expected, the absence of UV-accelerated aging processes did not allow the detection of macroscopic changes at the molecular level. As previously described, we specifically selected VL irradiation to mimic real conditions. However, NTA and DLS data on MP suspensions revealed that light irradiation led to a reduction in the hydrodynamic diameter of the particles (Fig. 1). Additionally, NTA indicated an increase in particle concentration after light exposure (Section 3.2). These findings suggest that even mild irradiation of the PS-MPs particles may cause their partial fragmentation, that could result in the possible release of nanoparticles in the water solution. It has been demonstrated that several nanoparticles are able to interact with the organic components of the cell medium, giving rise to the formation of a protein corona on the particle surface, which causes the size of the particle to increase (Mugnano et al., 2020). Therefore, understanding the polydispersity of the PS-MPs vs PS-MPs^{3h} particles in cell culture media, where a protein corona could coat the nanoparticle's surface, it is relevant for our study since these properties can influence the nanoparticle's interaction with cell targets. In this experimental setup, we observed that PS-MPs suspended in cell culture medium tended to cluster, exhibiting a size increase of approximately 30% compared to those in a water solution. (Fig. 1 panel c). Agglomeration of PS-MPs is likely due to the increased ionic strength of DMEM medium, which limits solvation of the polymer nanoparticles, causing them to coalesce and their hydrodynamic diameter to increase. The addition of FBS resulted in an increased size of pristine PS-MPs, suggesting enhanced desolvation and agglomeration of the particles. On the other hand, in the case of PS-MPs^{3h}, the size reduction (Fig. 1 panel d) suggests that the functional groups generated on the particle surface upon ageing could interact with the protein fraction of the medium, facilitating the solvation of the particle and possibly providing the latter with a new biological fingerprint. Starting from this scenario, we chose to compare the immunological responses elicited by irradiated PS-MPs^{3h} particles with those of pristine PS-MPs, aiming to understand the downstream immunological effects of solar irradiation on polystyrene microparticles. To accomplish this task, concentrations of PS-MPs and PS-MPs^{3h} microparticles derived from experimental determinations in biological samples were utilized in cell culture assays to study their effect on the inflammatory response of murine macrophages. In this setting, we demonstrated that a mild aging treatment together with experimentally determined concentration of PS nanoparticles can have an effect on the expression of markers of inflammatory macrophage response such as IL-6, NOS2 and ROS production. IL-6 is a cytokine with pleiotropic functions known to play a pivotal role in the regulation of immune responses in both physiological and pathological conditions including the activation and differentiation of various immune cells (Hirano, 2021). Its secretion is tightly regulated and can be induced by various stimuli, including ROS. On the other hand, IL-6 itself can also modulate ROS generation through various mechanisms, including the induction of antioxidant enzymes and the regulation of mitochondrial function leading to oxidative stress, causing damage to cellular components like proteins, lipids, and DNA (Di Meo et al., 2016). The interplay between ROS production and nitric oxide synthetase 2 can act as signalling molecules to induce the expression and activity of NOS2. NOS2 plays a significant role in the body's immune response by producing nitric oxide (NO) at elevated levels during inflammation. NO is a highly reactive free radical and serves as an important signalling molecule involved in immune regulation (Xue et al., 2018). However, the high output of NO can have deleterious effects, particularly on DNA integrity. This synergistic induction of NOS2 by ROS amplifies the inflammatory response and, in physiological conditions, contributes to host defence mechanisms against pathogens (Monteiro et al., 2019). Following this line of evidence, we evaluated the expression of γ-H2AX, a phosphorylated form of the histone variant H2AX, that becomes phosphorylated on serine 139 in response to DNA double-strand breaks particularly in response to DNA damage with particular reference to the reactive oxygen species. This phosphorylation event marks an early cellular response to DNA damage and serves as a signal for recruiting DNA repair mechanisms (Kopp et al., 2019). By means of immunofluorescence staining and Western blot analysis, we demonstrated that photoaging can also induced an increase in the expression of this marker of DSB upon PS-MPs^{3h} stimulation demonstrating that polystyrene aging can also induce dangerous genotoxic effects even at concentrations as low as 0.1 μg/ml, which are close to those experimentally evaluated in human biological samples.

5. Conclusion

The daily accumulation of information on the identification of environmentally derived microplastics in biological fluids raises several urgent questions regarding their effects on various ecosystems. Our data demonstrated that mild irradiation, mimicking solar irradiation, can indeed significantly affects the features of polystyrene microplastics and downstream modulate the activity of immune cells. This aspect can be a very relevant issue since, it has demonstrated that the shifts in the inflammatory response from short-to long-lived can cause a breakdown of immune tolerance and lead to major alterations in all tissues and organs (Kotas and Medzhitov, 2015; Fullerton and Gilroy, 2016). This highlights the need for further exploration to comprehend the potential detrimental effects of microplastics on the immunological mechanisms triggered by these particles.

Funding

G.C, S.C.E. and P.C. acknowledge support from the project PAPILLONS funded under European Union's Horizon 2020 research and innovation programme (grant agreement No 101000210). This publication reflects only the author's view and the European Commission is not responsible for any use that may be made of the information it contains.

CRediT authorship contribution statement

Noemi Aloi: Writing – original draft, Formal analysis. **Anna Calarco:** Formal analysis, Data curation. **Giusy Curcuruto:** Writing – original draft, Formal analysis. **Marilena Di Natale:** Conceptualization.

Giuseppa Augello: Formal analysis. **Sabrina Carola Carroccio:** Supervision. **Pierfrancesco Cerruti:** Supervision. **Melchiorre Cervello:** Supervision. **Angela Cuttitta:** Supervision. **Paolo Colombo:** Writing – review & editing, Writing – original draft, Supervision. **Valeria Longo:** Writing – original draft, Formal analysis.

Declaration of competing interest

The authors declare that they have no known competing financial interests or personal relationships that could have appeared to influence the work reported in this paper.

Data availability

Data will be made available on request.

Appendix A. Supplementary data

Supplementary data to this article can be found online at https://doi.org/10.1016/j.chemosphere.2024.143131.

References

Alfaro-Nunez, A., Astorga, D., Caceres-Farias, L., Bastidas, L., Soto Villegas, C., Macay, K., Christensen, J.H., 2021. Microplastic pollution in seawater and marine organisms across the tropical Eastern Pacific and Galapagos. Sci. Rep. 11, 6424.

Andrady, A.L., 2015. Marine Anthropogenic Litter||Persistence of Plastic Litter in the Oceans.

Argenziano, R., Agustin-Salazar, S., Panaro, A., Calarco, A., Di Salle, A., Aprea, P., Cerruti, P., Panzella, L., Napolitano, A., 2023. Combining the potent reducing properties of Pecan Nutshell with a solvent-free mechanochemical approach for synthesizing high Ag(0) content-silver nanoparticles: an eco-friendly route to an efficient multifunctional photocatalytic, antibacterial, and antioxidant material. Nanomaterials 13.

Baeza-Martinez, C., Olmos, S., Gonzalez-Pleiter, M., Lopez-Castellanos, J., Garcia-Pachon, E., Masia-Canuto, M., Hernandez-Blasco, L., Bayo, J., 2022. First evidence of microplastics isolated in European citizens' lower airway. J. Hazard Mater. 438, 129439.

Banerjee, A., Shelver, W.L., 2021. Micro- and nanoplastic induced cellular toxicity in mammals: a review. Sci. Total Environ. 755, 142518.

Cai, L., Wang, J., Peng, J., Wu, Z., Tan, X., 2018. Observation of the degradation of three types of plastic pellets exposed to UV irradiation in three different environments. Sci. Total Environ. 628–629, 740–747.

Carroccio, S., Puglisi, C., Montaudo, G., 2003. Photo-oxidation products of polyetherimide ULTEM determined by MALDI-TOF-MS. Kinetics and mechanisms. Polym. Degrad. Stabil. 80, 459–476.

Covello, C., Di Vincenzo, F., Cammarota, G., Pizzoferrato, M., 2024. Micro(nano)plastics and their potential impact on human gut health: a narrative review. Curr. Issues Mol. Biol. 46, 2658–2677.

Cox, K.D., Covernton, G.A., Davies, H.L., Dower, J.F., Juanes, F., Dudas, S.E., 2019. Human consumption of microplastics. Environ. Sci. Technol. 53, 7068–7074.

Cunningham, E.M., Seijo, N.R., Altieri, K.E., Audh, R.R., Burger, J.M., Bornman, T.G., Fawcett, S., Gwinnett, C.N.B., Osborne, A.O., Woodall, L.C., 2022. Microplastics pollution as an invisible potential threat to food safety and security, policy challenges and the way forward. Front. Mar. Sci.

Cusimano, A., Puleio, R., D'Alessandro, N., Loria, G.R., McCubrey, J.A., Montalto, G., Cervello, M., 2015. Cytotoxic activity of the novel small molecule AKT inhibitor SC66 in hepatocellular carcinoma cells. Oncotarget 6, 1707–1722.

Di Meo, S., Reed, T.T., Venditti, P., Victor, V.M., 2016. Role of ROS and RNS sources in physiological and pathological conditions. Oxid Med Cell Longev 2016, 1245049.

Di Natale, M.V., Carroccio, S.C., Dattilo, S., Cocca, M., Nicosia, A., Torri, M., Bennici, C. D., Musco, M., Masullo, T., Russo, S., Mazzola, A., Cuttitta, A., 2022. Polymer aging affects the bioavailability of microplastics-associated contaminants in sea urchin embryos. Chemosphere 309, 136720.

Eerkes-Medrano, D., Thompson, R.C., Aldridge, D.C., 2015. Microplastics in freshwater systems: a review of the emerging threats, identification of knowledge gaps and prioritisation of research needs. Water Res. 75, 63–82.

EFSA, 2021. Presence of microplastics and nanoplastics in food, withparticular focus on seafood. EFSA J. 14.

Eriksen, M., Lebreton, L.C., Carson, H.S., Thiel, M., Moore, C.J., Borerro, J.C., Galgani, F., Ryan, P.G., Reisser, J., 2014. Plastic pollution in the world's oceans: more than 5 trillion plastic pieces weighing over 250,000 tons afloat at sea. PLoS One 9, e111913.

Fan, J., Liu, L., Lu, Y., Chen, Q., Fan, S., Yang, Y., Long, Y., Liu, X., 2024. Acute exposure to polystyrene nanoparticles promotes liver injury by inducing mitochondrial ROS-dependent necroptosis and augmenting macrophage-hepatocyte crosstalk. Part. Fibre Toxicol. 21, 20.

Fleury, J.B., Baulin, V.A., 2021. Microplastics destabilize lipid membranes by mechanical stretching. Proc. Natl. Acad. Sci. U. S. A. 118.

Frank, E.A., Meek, M.E.B., 2024. Procedural application of mode-of-action and human relevance analysis: styrene-induced lung tumors in mice. Crit. Rev. Toxicol. 54, 134–151.

Fullerton, J.N., Gilroy, D.W., 2016. Resolution of inflammation: a new therapeutic frontier. Nat. Rev. Drug Discov. 15, 551–567.

Heddagaard, F.E., Moller, P., 2020. Hazard assessment of small-size plastic particles: is the conceptual framework of particle toxicology useful? Food Chem. Toxicol. 136, 111106.

Hirano, T., 2021. IL-6 in inflammation, autoimmunity and cancer. Int. Immunol. 33, 127–148.

Hodson, M.E., Duffus-Hodson, C.A., Clark, A., Prendergast-Miller, M.T., Thorpe, K.L., 2017. Plastic bag derived-microplastics as a vector for metal exposure in terrestrial invertebrates. Environ. Sci. Technol. 51, 4714–4721.

Horton, A.A., Svendsen, C., Williams, R.J., Spurgeon, D.J., Lahive, E., 2017. Large microplastic particles in sediments of tributaries of the River Thames, UK - abundance, sources and methods for effective quantification. Mar. Pollut. Bull. 114, 218–226.

Hou, B., Wang, F., Liu, T., Wang, Z., 2021. Reproductive toxicity of polystyrene microplastics: in vivo experimental study on testicular toxicity in mice. J. Hazard Mater. 405, 124028.

Huang, Y., Ding, J., Zhang, G., Liu, S., Zou, H., Wang, Z., Zhu, W., Geng, J., 2021. Interactive effects of microplastics and selected pharmaceuticals on red tilapia: role of microplastic aging. Sci. Total Environ. 752, 142256.

Jeon, S., Jeon, J.H., Jeong, J., Kim, G., Lee, S., Kim, S., Maruthupandy, M., Lee, K., Yang, S.I., Cho, W.S., 2023. Size- and oxidative potential-dependent toxicity of environmentally relevant expanded polystyrene styrofoam microplastics to macrophages. J. Hazard Mater. 459, 132295.

Jin, H., Ma, T., Sha, X., Liu, Z., Zhou, Y., Meng, X., Chen, Y., Han, X., Ding, J., 2021. Polystyrene microplastics induced male reproductive toxicity in mice. J. Hazard Mater. 401, 123430.

Kopp, B., Khoury, L., Audebert, M., 2019. Validation of the gammaH2AX biomarker for genotoxicity assessment: a review. Arch. Toxicol. 93, 2103–2114.

Kotas, M.E., Medzhitov, R., 2015. Homeostasis, inflammation, and disease susceptibility. Cell 160, 816–827.

Kumar, M., Chen, H., Sarsaiya, S., Qin, S., Liu, H., Awasthi, M.K., Kumar, S., Singh, L., Zhang, Z., Bolan, N.S., Pandey, A., Varjani, S., Taherzadeh, M.J., 2021. Current research trends on micro- and nano-plastics as an emerging threat to global environment: a review. J. Hazard Mater. 409, 124967.

Kuo, L.J., Yang, L.X., 2008. Gamma-H2AX - a novel biomarker for DNA double-strand breaks. In Vivo 22, 305–309.

Lee, J.H., Park, E., Jin, H.J., Lee, Y., Choi, S.J., Lee, G.W., Chang, P.S., Paik, H.D., 2017. Anti-inflammatory and anti-genotoxic activity of branched chain amino acids (BCAA) in lipopolysaccharide (LPS) stimulated RAW 264.7 macrophages. Food Sci. Biotechnol. 26, 1371–1377.

Leslie, H.A., van Velzen, M.J.M., Brandsma, S.H., Vethaak, A.D., Garcia-Vallejo, J.J., Lamoree, M.H., 2022. Discovery and quantification of plastic particle pollution in human blood. Environ. Int. 163, 107199.

Liu, P., Zhang, Y., Gao, Z., Li, Z., 2019. Study on photodegradation pathway and mechanism of 2,2′,4,4′-Tetrabromodiphenyl ether. Emerging Contam. 5, 45–52.

Mao, R., Lang, M., Yu, X., Wu, R., Yang, X., Guo, X., 2020. Aging mechanism of microplastics with UV irradiation and its effects on the adsorption of heavy metals. J. Hazard Mater. 393, 122515.

Monteiro, H.P., Rodrigues, E.G., Amorim Reis, A.K.C., Longo Jr., L.S., Ogata, F.T., Moretti, A.I.S., da Costa, P.E., Teodoro, A.C.S., Toledo, M.S., Stern, A., 2019. Nitric oxide and interactions with reactive oxygen species in the development of melanoma, breast, and colon cancer: a redox signaling perspective. Nitric Oxide 89, 1–13.

Mugnano, M., Lama, G.C., Castaldo, R., Marchesano, V., Merola, F., del Giudice, D., Calabuig, A., Gentile, G., Ambrogi, V., Cerruti, P., Memmolo, P., Pagliarulo, V., Ferraro, P., Grilli, S., 2020. Cellular uptake of mildly oxidized nanographene for drug-delivery applications. ACS Appl. Nano Mater. 3, 428–439.

Park, J., Kim, Y.S., Hammond, P.T., 2005. Chemically nanopatterned surfaces using polyelectrolytes and ultraviolet-cured hard molds. Nano Lett. 5, 1347–1350.

Rodrigues, J., Duarte, A., Santos-Echeandía, J., Rocha-Santos, T., 2019. Significance of interactions between microplastics and POPs in the marine environment: a critical overview. Trends Anal. Chem. 111, 252–260.

Santillo, D., Miller, K., Johnston, P., 2017. Microplastics as contaminants in commercially important seafood species. Integrated Environ. Assess. Manag. 13, 516–521.

Schwabl, P., Koppel, S., Konigshofer, P., Bucsics, T., Trauner, M., Reiberger, T., Liebmann, B., 2019. Detection of various microplastics in human stool: a prospective case series. Ann. Intern. Med. 171, 453–457.

Sewwandi, M., Wijesekara, H., Rajapaksha, A.U., Soysa, S., Vithanage, M., 2023. Microplastics and plastics-associated contaminants in food and beverages; Global trends, concentrations, and human exposure. Environ. Pollut. 317, 120747.

Shaddick, G., Ranzi, A., Thomas, M.L., Aguirre-Perez, R., Dunbar Bekker-Nielsen, M., Parmagnani, F., Martuzzi, M., 2018. Towards an assessment of the health impact of industrially contaminated sites: waste landfills in Europe. Epidemiol. Prev. 42, 69–75.

Soni, S.S., Kim, K.M., Sarkar, B., Rodell, C.B., 2024. Uptake of cyclodextrin nanoparticles by macrophages is dependent on particle size and receptor-mediated interactions. ACS Appl. Bio Mater.

Urso, M., Ussia, M., Novotny, F., Pumera, M., 2022. Trapping and detecting nanoplastics by MXene-derived oxide microrobots. Nat. Commun. 13, 3573.

Usman, S., Abdull Razis, A.F., Shaari, K., Amal, M.N.A., Saad, M.Z., Mat Isa, N., Nazarudin, M.F., Zulkifli, S.Z., Sutra, J., Ibrahim, M.A., 2020. Microplastics pollution

as an invisible potential threat to food safety and security, policy challenges and the way forward. Int. J. Environ. Res. Publ. Health 17.
Visentin, E., Manuelian, C.L., Niero, G., Benetti, F., Perini, A., Zanella, M., Pozza, M., De Marchi, M., 2024. Characterization of microplastics in skim-milk powders. J. Dairy Sci.
Wagner, M., Scherer, C., Alvarez-Munoz, D., Brennholt, N., Bourrain, X., Buchinger, S., Fries, E., Grosbois, C., Klasmeier, J., Marti, T., Rodriguez-Mozaz, S., Urbatzka, R., Vethaak, A.D., Winther-Nielsen, M., Reifferscheid, G., 2014. Microplastics in freshwater ecosystems: what we know and what we need to know. Environ. Sci. Eur. 26, 12.
Wang, J., Tan, Z., Peng, J., Qiu, Q., Li, M., 2016. The behaviors of microplastics in the marine environment. Mar. Environ. Res. 113, 7–17.
Wright, S.L., Kelly, F.J., 2017. Plastic and human health: a micro issue? Environ. Sci. Technol. 51, 6634–6647.
Xue, Q., Yan, Y., Zhang, R., Xiong, H., 2018. Regulation of iNOS on immune cells and its role in diseases. Int. J. Mol. Sci. 19.
Yang, W., Jannatun, N., Zeng, Y., Liu, T., Zhang, G., Chen, C., Li, Y., 2022. Impacts of microplastics on immunity. Front Toxicol 4, 956885.
Yin, K., Wang, D., Zhang, Y., Lu, H., Hou, L., Guo, T., Zhao, H., Xing, M., 2023. Polystyrene microplastics promote liver inflammation by inducing the formation of macrophages extracellular traps. J. Hazard Mater. 452, 131236.